Available online at www.sciencedirect.com
SCIENCE DIRECT®
Journal of Solid State Chemistry 174 (2003) 329–333
JOURNAL OF SOLID STATE CHEMISTRY
http://elsevier.com/locate/jssc

# The synthesis, crystal chemistry and structures of Y-doped brannerite ($U_{1-x}Y_xTi_2O_6$) and thorutite ($Th_{1-x}Y_xTi_2O_{6-\delta}$) phases

M. James,[a,*] M.L. Carter,[b] and J.N. Watson[a]

[a] *The Bragg Institute, Australian Nuclear Science and Technology Organisation (ANSTO), PMB 1 Menai NSW 2234, Australia*
[b] *Materials and Engineering Science, Australian Nuclear Science and Technology Organisation (ANSTO), PMB 1, Menai NSW 2234, Australia*

Received 7 November 2002; received in revised form 14 April 2003; accepted 25 April 2003

**Abstract**

Yttrium-doped uranium brannerite ($U_{1-x}Y_xTi_2O_6$) and thorutite ($Th_{1-x}Y_xTi_2O_{6-\delta}$) phases were synthesized in air at 1400°C. Powder X-ray diffraction revealed that these phases crystallized to form monoclinic ($C2/m$) structures. Crystal structures of $U_{0.54}Y_{0.46}Ti_2O_6$ (**1**) ($a = 9.8008(2)$; $b = 3.7276(1)$; $c = 6.8745(1)$; $\beta = 118.38(1)$; $V = 220.97(1)$; $Z = 2$; $R_P = 7.3\%$; $R_B = 4.6\%$) and $Th_{0.91}Y_{0.09}Ti_2O_{6-\delta}$ (**2**) ($a = 9.8002(7)$; $b = 3.7510(3)$; $c = 6.9990(5)$; $\beta = 118.37(4)$; $V = 226.40(3)$; $Z = 2$; $R_P = 4.5\%$; $R_B = 2.9\%$) were refined from powder neutron diffraction data. These two phases were isostructural, revealing planes of corner and edge-sharing $TiO_6$ octahedra separated by irregular eight-fold coordinate U/Y or Th/Y atoms. The oxygen sites within the structure of **1** were found to be fully occupied, confirming that the doping of lower valence Y atoms occurs in conjunction with the oxidation of U(IV) to U(V). Y doping of the thorutite phase **2** does not lead to oxidation but rather the formation of oxygen vacancies within the structure.
© 2003 Elsevier Science (USA). All rights reserved.

*Keywords:* Doped uranium brannerite; Powder neutron diffraction; Rietveld refinement; Nuclear waste immobilization

## 1. Introduction

Brannerite, $UTi_2O_6$, has been found to be present as a minor phase in titanate-based pyrochlore-rich ceramics of the synroc [1] type designed for the geological immobilization of excess weapons Pu [2,3]. Brannerite in these ceramics was found to incorporate neutron absorbers such as Gd and Hf as well as Pu and U. The neutron absorbers are present in these ceramics to overcome potential criticality problems associated with the presence of Pu.

Natural brannerite occurs as a mineral that is nearly always X-ray amorphous because of radiation damage from α-decay of U, Th and daughter isotopes. Crystalline forms of brannerite having a monoclinic structure have been produced either by recrystallization at ~1000°C [4,5] or by synthesis under low-oxygen conditions [4]. Furthermore, it has recently been shown that incorporation of other divalent, trivalent and tetravalent dopants provides a means of stabilising brannerite phases produced in air [6,7].

The present work examines the substitutional chemistry of brannerite ($UTi_2O_6$) and thorutite ($ThTi_2O_6$) phases as a function of yttrium doping to form $U/Th_{1-x}Y_xTi_2O_6$. We report structural changes as a function of Y-content and in particular describe the structures of $U_{0.54}Y_{0.46}Ti_2O_6$ (**1**) and $Th_{0.91}Y_{0.09}Ti_2O_{6-\delta}$ (**2**) as determined by powder neutron diffraction.

## 2. Experimental

### 2.1. Synthesis

The samples were prepared by the alkoxide/nitrate route [8]; the mixtures dried and calcined in air at 750°C for 1 h. The calcines were wet milled for 16 h and dried before cold pressing and firing the pellets for 14 h at 1400°C under air.

### 2.2. Electron microscopy

Scanning electron microscopy (SEM) was carried out with a JEOL 6400 instrument run at 15 kV, and fitted with a Tracor Northern TN5502 energy-dispersive

*Corresponding author. Fax: +61-2-9717-3606.
*E-mail address:* mja@ansto.gov.au (M. James).

0022-4596/03/$ - see front matter © 2003 Elsevier Science (USA). All rights reserved.
doi:10.1016/S0022-4596(03)00230-5

X-ray (EDX) detector, which utilized a comprehensive set of standards for quantitative work.

### 2.3. Diffraction measurements

Powder X-ray diffraction measurements were made on a Scintag Inc. XGEN 4000 X-ray diffractometer at ambient temperature using Cu$K\alpha$ radiation and a flat-plate sample holder. Data of sufficient quality for structural refinement were collected over $5° < 2\Theta < 85°$, in 0.025° steps, with integration times of 10 s. Powder neutron diffraction measurements were also made on the high-resolution powder diffractometer (HRPD) using thermal neutrons ($\lambda = 1.4930$ Å (**1**), 1.8855 Å (**2**)) from the HIFAR nuclear reactor at ANSTO [9]. Data was collected using a bank of 24 $^3$He detectors over the range $10° < 2\Theta < 140°$, in 0.05° steps, with the measurement of **1** taking 44 h and **2** taking 32 h. Structural refinements were carried out by the Rietveld method [10] using the RIETICA program [11], with pseudo-Voigt peak shapes and refined backgrounds. Further details of the crystal structure investigation(s) can be obtained from the Fachinformationszentrum Karlsruhe, 76344 Eggenstein-Leopoldshafen, Germany (fax: +49-7247-808-66; mailto: crysdata@fiz-karlsruhe.de) on quoting the depository numbers CSD-412851 for **1** and CSD-412852 for **2**.

## 3. Results and discussion

### 3.1. Crystal chemistry and solid solution range

Our previous work indicated that sintering the correct stoichiometry in argon produced single-phase brannerite $UTi_2O_6$, however sintering in air produced $U_3O_8$ and $TiO_2$. Brannerite phases were also stabilized in an air atmosphere at high temperatures by substitution of $Ca^{2+}$ or lanthanide ions for $U^{4+}$ with oxidation of the remaining uranium to $U^{5+}$ [6,7].

As was the case for the doped $U_{1-x}M_xTi_2O_6$ phases [7], the solid solution range of $U_{1-x}Y_xTi_2O_6$ depends on the firing atmosphere. Under-doped samples prepared in air gave rise to brannerite phases, $U_3O_8$ and $TiO_2$ impurities, while over-doped samples contained brannerite phases, $TiO_2$ and pyrochlore phases ($Y_{1+x}U_{1-x}Ti_2O_7$). Over-doped samples of thorutite gave rise to $Th_{0.91}Y_{0.09}Ti_2O_{6-\delta}$ as well as the impurities $ThO_2$ and Y-rich $Y_2Ti_2O_7$. SEM and EDX analysis were used to characterize the solid solution range for the $U_{1-x}Y_xTi_2O_6$ phases formed at 1400°C. $U_{1-x}Y_xTi_2O_6$ showed a similar solid solution range ($0.29 \leqslant x \leqslant 0.46$), to other rare earth doped brannerite phases prepared in air ($La^{3+}$: $0.38 \leqslant x \leqslant 0.50$ and $Gd^{3+}$: $0.31 \leqslant x \leqslant 0.50$), and a more extensive range than calcium-doped brannerite ($0.21 \leqslant x \leqslant 0.28$) [7]. It is assumed that no oxygen vacancies are produced in $U_{1-x}Y_xTi_2O_6$ and that U(IV) is oxidized to U(V) in order to compensate for the introduction of $Y^{3+}$. Thus, sintering of $U_{1-x}Y_xTi_2O_6$ in air gave rise to $(^x/_{(1-x)})$ U(V) (i.e. between 41% and 87%).

In contrast, the solid solution range for Y-doped $ThTi_2O_6$ was found to be far more restricted than observed for $U_{1-x}Y_xTi_2O_6$ with a lower limit of 0 and an upper limit of only 0.09. With only a ~3% difference in ionic radii between $Th^{4+}$ and $Y^{3+}$, there is little suggestion that size differences are the major factor in the limited solid solution range. The key lies more with the inability of thorium to be oxidized beyond Th(IV). This is not a surprise given that synthetic or natural compounds having oxidation states of Th(V) or higher have not been previously reported. Thus, the only mechanism of charge balance is via oxygen vacancy formation and unlike brannerite, doping of thorutite by $Y^{3+}$ does not lead to the oxidation of Th(IV) to Th(V).

As was found to be the case for doped brannerite phases $U_{1-x}M_xTi_2O_6$ ($M = Ca^{2+}$, $La^{3+}$, and $Gd^{3+}$) [7], other rare earth ions such as $Gd^{3+}$ were also found to substitute for $Th^{4+}$ in $ThTi_2O_6$ at similar levels to that observed for $Th_{0.91}Y_{0.09}Ti_2O_{6-\delta}$. Unlike the doped brannerite materials however, $Ca^{2+}$ was not found to substitute into $ThTi_2O_6$.

## 4. Structural refinements

### 4.1. X-ray diffraction profiles

In each case the X-ray diffraction patterns of $U_{1-x}Y_xTi_2O_6$ could be indexed based on the monoclinic $C2/m$ cell of uranium brannerite $UTi_2O_6$ [4]. Attempts to refine the structures of these phases using the structure of $UTi_2O_6$ as an initial model were however unsuccessful, leading to very high residuals ($R_p \sim 20\%$) or unstable refinements. Comparison of the observed diffraction profiles with those calculated from idealized structures based on $UTi_2O_6$ indicated strong preferred orientation of the crystallites. Refinement of the Dollase preferred orientation function [12] along different directions did not lead to significant improvements in the fit to the data. Examination of the refined structures revealed significant 'non-physical' distortions, serving to highlight the difficulty in modelling substantial preferred orientation when using flat-plate Bragg–Brentano powder X-ray diffraction data. Unit-cell parameters were however able to be extracted from the powder X-ray diffraction data using the RIETICA program and the Le Bail method [13].

### 4.2. Neutron diffraction profiles

Due to the difference in scattering geometry, preferred orientation concerns were removed from the structural refinements when powder neutron diffraction data were used. Neutron diffraction data have the additional benefit of providing increased contrast with respect to the oxygen atoms than could be obtained by XRD, particularly given the presence of heavy atoms such as yttrium, thorium and uranium.

The structural parameters for **1** and **2** were determined by Rietveld refinement using the RIETICA program in space group $C2/m$ with Y and U/Th disordered over the 8 coordinate actinide $2a$ (0,0,0) sites (Table 1). The diffraction profiles for **1** revealed essentially a phase pure sample, although closer examination revealed a small amount of Y/U pyrochlore; this being consistent with the proximity of the sample to the phase boundary. Attempts were made to refine the Y/U ratio, however strong correlations were found to exist between the Y/U site occupancies and the isotropic thermal parameter. Therefore, the site occupancies of Y and U were set at their composition as determined by EDX (0.46 and 0.54, respectively). In the final stages of the refinement the occupancy of the oxygen sites of **1** were refined and were found to be fully occupied; this being consistent with the oxidation of U(IV) to U(V) and no formation of oxygen vacancies. The pyrochlore impurity was included as a second phase in the structural model, leading to a noticeable improvement in the quality of the refinement ($R_p \sim 5.9\% \rightarrow R_p \sim 4.9\%$). The refined molar fraction of pyrochlore was determined as 2.1(1)%. The observed, calculated and difference diffraction profiles for **1** and **2** are shown in Figs. 1(a) and (b), respectively.

Table 1 contains crystallographic information extracted from powder diffraction data for end-member compositions of $U_{1-x}Y_xTi_2O_6$ and **2**. Examination of Table 1 reveals the effect of doping on the brannerite structure. Replacing $U^{4+}$ having an ionic radius of 1.00 Å [14], by the slightly larger $Y^{3+}$ ion (1.019 Å) in $U_{0.54}Y_{0.46}Ti_2O_6$ is off-set by the oxidation of the remaining uranium to the smaller (0.89 Å) $U^{5+}$. The doping and subsequent oxidation leads to a contraction in the unit cell from 224.1(1) $Å^3$ as present in $UTi_2O_6$ (1) to 219.12(1) $Å^3$ in $U_{0.54}Y_{0.46}Ti_2O_6$. Refined atomic positions and thermal parameters are given in Table 2 and the refined structure (of **1**) is displayed in Fig. 2. Selected bond lengths are displayed in Table 3.

As has been observed in numerous perovskite-based compounds, significant variation in ionic size or charge can lead to ordering of the individual ionic species onto distinct crystallographic sites along with an accompanying change in unit-cell dimensions (i.e., the formation of a super-lattice structure). Careful examination of the neutron and X-ray diffraction profiles of both did not

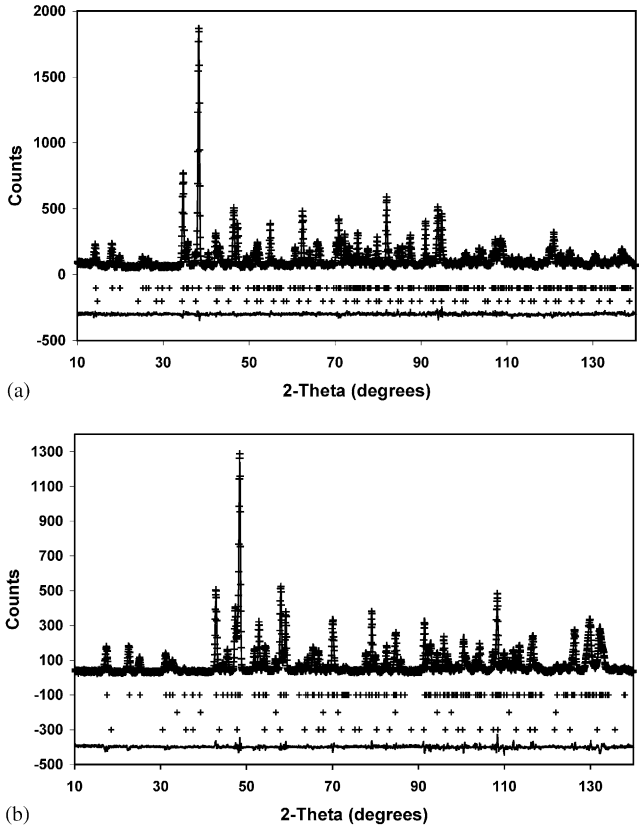


Fig. 1. The observed (crosses), calculated and difference (solid lines) powder neutron diffraction profiles for (a) $U_{0.54}Y_{0.46}Ti_2O_6$ (**1**) and (b) $Th_{0.91}Y_{0.09}Ti_2O_{6-\delta}$ (**2**).

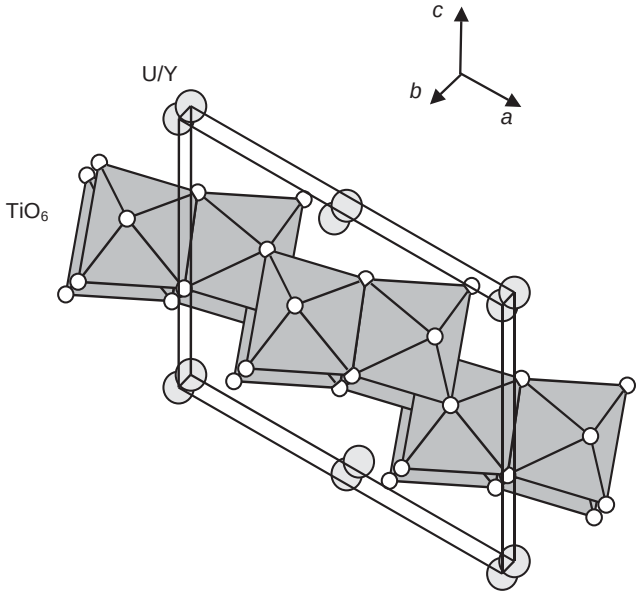


Fig. 2. The refined crystal structure of $U_{0.54}Y_{0.46}Ti_2O_6$ (**1**), showing sheets of corner and edge-sharing $TiO_6$ octahedra along the *ab* plane and eight-fold coordinate U/Y atoms between the planes.

Table 1
Crystallographic data for $U_{0.71}Y_{0.29}Ti_2O_6$, $U_{0.54}Y_{0.46}Ti_2O_6$ (**1**) and $Th_{0.91}Y_{0.09}Ti_2O_{6-\delta}$ (**2**)

| Formula | $U_{0.71}Y_{0.29}Ti_2O_6$ | $U_{0.54}Y_{0.46}Ti_2O_6$ | $Th_{0.91}Y_{0.09}Ti_2O_{6-\delta}$ |
|---|---|---|---|
| Formula weight | 386.543 | 355.227 | 409.485 |
| Color | Black | Black | Black |
| $U^{4+}$:$U^{5+}$ (%) | 59:41 | 13:87 | |
| Space group | $C2/m$ (No. 12) | $C2/m$ | $C2/m$ |
| $Z$ | 2 | 2 | 2 |
| $a$ (Å) | 9.818(2)[a] | 9.8039(2)[b] | 9.8176(2)[b] |
| $b$ (Å) | 3.731(1)[a] | 3.7188(1)[b] | 3.8141(1)[b] |
| $c$ (Å) | 6.876(2)[a] | 6.8403(2)[b] | 6.8271(3)[b] |
| $\beta$ (deg) | 118.68(1)[a] | 118.52(1)[b] | 118.74(1)[b] |
| $V$ (Å$^3$) | 221.0(1)[a] | 219.12(1)[b] | 230.47(1)[b] |
| $\rho_{calc}$ (g cm$^{-3}$) | 5.809[a] | 5.382[b] | 5.899[b] |
| $2\theta$ range (deg) | 5–85[a] | 10–140[b] | 10–140[b] |
| $\lambda$ (Å) | 1.5406[a] | 1.4930[b] | 1.8855[b] |
| No. of reflns | 98[a] | 279[b] | 148[b] |
| $R_P/R_B$ | | 4.9%/2.2%[b] | 6.6%/3.0%[b] |

[a] As determined from powder X-ray diffraction data using the Le Bail method [14].
[b] As determined from powder neutron diffraction data using the Rietveld method [11].

Table 2
Fractional atomic coordinates and equivalent isotropic thermal parameters ($B_{eq}$) (Å$^2 \times 100$) for $U_{0.54}Y_{0.46}Ti_2O_6$ and $Th_{0.91}Y_{0.09}Ti_2O_{6-\delta}$ with Esd's in parentheses, as determined from powder neutron diffraction data

| | $U_{0.54}Y_{0.46}Ti_2O_6$ | $Th_{0.91}Y_{0.09}Ti_2O_{6-\delta}$ |
|---|---|---|
| Y/U/Th (2*a*) | | |
| *x* | 0 | 0 |
| *y* | 0 | 0 |
| *z* | 0 | 0 |
| $B_{eq}$ | 1.0(1) | 1.5(1) |
| Occ (Y) | 0.46 | 0.09 |
| Occ (U/Th) | 0.54 | 0.91 |
| Ti (4*i*) | | |
| *x* | 0.8261(4) | 0.8265(4) |
| *y* | 0 | 0 |
| *z* | 0.3922(6) | 0.3980(4) |
| $B_{eq}$ | 0.6(1) | 0.5(1) |
| O1 (4*i*) | | |
| *x* | 0.9785(2) | 0.9782(2) |
| *y* | 0 | 0 |
| *z* | 0.3061(3) | 0.3140(4) |
| $B_{eq}$ | 0.9(1) | 0.7(1) |
| O2 (4*i*) | | |
| *x* | 0.6509(2) | 0.6563(3) |
| *y* | 0 | 0 |
| *z* | 0.1034(3) | 0.1109(4) |
| $B_{eq}$ | 1.1(1) | 0.8(1) |
| O3 (4*i*) | | |
| *x* | 0.2835(2) | 0.2820(2) |
| *y* | 0 | 0 |
| *z* | 0.4072(3) | 0.4083(3) |
| $B_{eq}$ | 1.1(1) | 0.9(1) |

provide any evidence for cation ordering in these phases, despite the substantial charge difference between $Y^{3+}$ and $U^{5+}$ and the (~15%) difference in their ionic radii.

The structure of **2** was also refined in a similar fashion from powder neutron diffraction data and was found to be essentially isostructural with **1** with Y and Th disordered over the 2*a* sites. As was the case of **1** strong correlations prevented refinement of the Y/Th site occupancies. The oxygen site occupancies were also refined and were not found to differ significantly from unity (i.e., they appear to be fully occupied). This result although appearing contrary to the notion of oxygen vacancies, is not unexpected. Given the amounts of $Y^{3+}$ and $Th^{4+}$ (as determined by SEM) the oxygen vacancy level is expected to be $\delta \sim 0.045$. With three oxygen sites in the structure, the occupancies with an average vacancy level would only be 0.993. This small vacancy level is beyond the capability to be detected by Rietveld refinement based on neutron diffraction data. In addition to the main phase, small amounts of $ThO_2$ (3.7%) and $Y_2Ti_2O_7$ (1.6%) were observed to be present. The refined cell dimensions of **2** (Table 1) were found to be slightly smaller ($V = 230.47(1)$ Å$^3$) than those for $ThTi_2O_6$ ($V = 231.12(1)$ Å$^3$) [15]. This is reasonable given that eight-fold coordinate $Y^{3+}$ (1.019 Å) is slightly smaller than eight-fold coordinate $Th^{4+}$ (1.05 Å).

The structures of both $U_{0.54}Y_{0.46}Ti_2O_6$ and $Th_{0.91}Y_{0.09}Ti_2O_{6-\delta}$ consist of sheets of corner and edge sharing, $TiO_6$ octahedra in the *ab* plane (Fig. 2). The U/Th/Y atoms adopt an irregular eight-fold coordination between these sheets. The average Ti–O bond lengths in **1** (1.956(2) Å) and **2** (1.963(3) Å) are slightly shorter than those typically observed by Shannon (2.005 Å) for other oxides of Ti(IV) [14]. In addition, within each $TiO_6$ octahedron there is significant variation of Ti–O bond lengths (Table 3), reflecting an irregular coordination. In **1**, where octahedra share a common edge, the average distance between adjacent oxygen atoms is 2.49 Å, while the average distance between corner-sharing oxygen atoms is substantially longer at 2.90 Å. The average observed U–O bond length for **1** (2.396 Å) appears slightly longer than expected from other uranium containing oxides (2.36 Å) [14]. It is however an artifact of the highly asymmetric coordination sphere. Examination of Table 3 and Fig. 2 reveals three distinct types of U/Y–O bonds: a pair of short U/Y–O1 bonds (2.203(2) Å), four short bonds (2.269(1) Å) to O2 atoms that bridge pairs of U/Y atoms along the *b*-axis and a pair of long U/Y–O3 bonds (2.844 Å). By way of comparison, the equivalent bond lengths in $UTi_2O_6$ were found to be 2.252, 2.296 and 2.824 Å for U–O1, U–O2 and U–O3, respectively [4]. The underlying asymmetric nature of the U/Y coordination sphere in each of these cases is therefore not a

Table 3
Selected bond lengths (Å) for $U_{0.54}Y_{0.46}Ti_2O_6$ and $Th_{0.91}Y_{0.09}Ti_2O_{6-\delta}$ as determined from powder neutron diffraction data

| | $U_{0.54}Y_{0.46}Ti_2O_6$ | $Th_{0.91}Y_{0.09}Ti_2O_{6-\delta}$ |
|---|---|---|
| U/Th–O1 (×2) | 2.203(2) | 2.314(2) |
| U/Th–O2 (×4) | 2.269(1) | 2.334(2) |
| U/Th–O3 (×2) | 2.844(2) | 2.872(2) |
| Ti–O1 | 1.849(2) | 1.847(5) |
| Ti–O1 | 2.038(3) | 2.010(3) |
| Ti–O2 | 1.901(3) | 1.901(2) |
| Ti–O3 | 2.108(2) | 2.092(3) |
| Ti–O3 (×2) | 1.919(1) | 1.965(1) |

consequence of Y-doping. Asymmetric Y–O bond lengths have however also been observed in other eight-fold coordinate titanates such as $Y_2Ti_2O_7$, with two short bonds (2.186 Å) and six long bonds (2.510 Å) [16]. Similar behavior is observed for **2** with a range of Y/Th–O bond lengths (2.314(2)—2.872(2) Å), however the average observed Y/Th–O bond length for **2** (2.464 Å) is very close to that expected from other thorium based oxides (2.46 Å) [14].

## 5. Bond valence sums

The valence of a site ($i$) may be calculated by the following expression:

$$V_i = \sum_j \exp((r_0 - r_{ij})/B),$$

where $r_{ij}$ are the observed bond lengths (Table 3), $B = 0.37$ and values of $r_0$ are those of Brown and Altermatt [17], with the exception of that for $U^{5+}$–O (2.094 Å), which we determined as the average of those for $U^{4+}$–O and $U^{6+}$–O. Bond valence values were calculated based on the quantities of $Y^{3+}$, $U^{4+}$, $U^{5+}$ and $Th^{4+}$ as listed in Table 1, giving 4.0(1) for the $Y^{3+}/U^{4+}/U^{5+}$ sites of **1** and 4.1(1) for the $Y^{3+}/Th^{4+}$ sites of **2**, respectively. Calculation of the Ti valence using the observed Ti–O bond lengths (Table 3) gave 4.2(1) and 4.1(1) for **1** and **2** respectively. In all cases the bond valence calculations for the different sites shows very good agreement with the expected site valences, despite the large amount of structural asymmetry observed for both the U(Th)/Y and Ti sites.

## 6. Conclusions

We have synthesized Y-doped uranium brannerite and thorutite phases $U_{1-x}Y_xTi_2O_6$ and $Th_{1-x}Y_xTi_2O_{6-\delta}$ at 1400°C in air. The range of solid solution of the former ($0.29 < 0.46$) was found to be similar to that observed for other rare earth doped brannerites; while yttrium-doped thorutite was found to have only a limited range (up to $x = 0.09$). Each of the phases produced was found to form a monoclinic structure. Rietveld refinement of powder neutron diffraction data for $U_{0.54}Y_{0.46}Ti_2O_6$ (**1**) confirms that doping of lower valence $Y^{3+}$ atoms into brannerite occurs in conjunction with the oxidation of U(IV) to U(V). Although not directly observed from the structural refinements in the case of $Th_{0.91}Y_{0.09}Ti_2O_{6-\delta}$ (**2**), we propose that a small number of oxygen vacancies ($\delta \sim 0.045$) were produced and thorium was not oxidized beyond Th(IV).

## References

[1] A.E. Ringwood, S.E. Kesson, N.G. Ware, W. Hibberson, A. Major, Nature (London) 278 (1979) 219–223.
[2] B.B. Ebbinghaus, R.A. VanKonynenburg, F.J. Ryerson, E.R. Vance, M.W.A. Stewart, A. Jostsons, J.S. Allender, T. Rankin, J. Congdon, Ceramic formulation for the immobilization of plutonium, Waste Management '98 (CD-ROM), Tucson, AZ, USA, March 5, 1998.
[3] E.R. Vance, M.W.A. Stewart, R.A. Day, K.P. Hart, M.J. Hambley, A. Brownscombe, pyrochlore-rich titanate ceramics for incorporation of plutonium, uranium and process chemicals, ANSTO Report, 1997.
[4] J.T. Szymanski, J.D. Scott, Canad. Mineral. 20 (1982) 271–279.
[5] J.E. Patchett, E.W. Nuffield, Canad. Mineral. 6 (1960) 483–490.
[6] E.R. Vance, J.N. Watson, M.L. Carter, R.A. Day, B.D. Begg, J. Am. Ceram. Soc. 84 (2001) 141–144.
[7] M. James, J.N. Watson, J. Solid State Chem. 165 (2001) 261–265.
[8] A.E. Ringwood, S.E. Kesson, K.D. Reeve, D.M. Levins, E.J. Ramm, in: W. Lutze, R.C. Ewing (Eds.), Radioactive Waste Forms for the Future, "Synroc", Elsevier, Amsterdam, Netherlands, 1988, pp. 223–334.
[9] S.J. Kennedy, Adv. X-ray Anal. 38 (1995) 35–46.
[10] H.M. Rietveld, J. Appl. Crystallogr. 2 (1969) 65–71.
[11] B.A. Hunter, Rietica—A Visual Rietveld Program in Commission on Powder Diffraction Newsletter, Vol. 20, 1998, p. 21; Available at: http://www.iucr.org/iucr-top/comm/cpd/Newsletters/
[12] W.A. Dollase, J. Appl. Crystallogr. 19 (1986) 267–272.
[13] A. Le Bail, H. Duroy, J.L. Fourquet, Mater. Res. Bull. 23 (1988) 447–452.
[14] R.D. Shannon, Acta Crystallogr. A 32 (1976) 751–767.
[15] R.H. Mitchell, A.R. Chakhmouradian, Phys. Chem. Minerals 26 (1999) 396–405.
[16] E. Chtoun, L. Hanebali, P. Garnier, J.M. Kiat, Eur. J. Solid State Inorg. Chem. 34 (1997) 553–561.
[17] D. Brown, D. Altermatt, Acta Crystallogr. B 41 (1985) 244–247.